Journal of Ceramic Processing Research. Vol. 14, No. 3, pp. 284~287 (2013)

J O U R N A L O F
Ceramic Processing Research

Effect of electrolyte concentration on the structural and optical properties of ZnO nanodisks formed on indium-tin-oxide coated glass substrates

Young Soo No[a], Hee Yeon Yang[b], Jin Young Kim[c] and Tae Whan Kim[a,b,*]

[a]*Department of Electronics and Computer Engineering, Hanyang University, Seoul, 133-791, Korea*
[b]*Department of Information Display Engineering, Hanyang University, Seoul, 133-791, Korea*
[c]*Department of Electronic Materials Engineering, Kwangwoon University, Seoul, 139-701, Korea*

ZnO nanodisks on indium-tin-oxide film coated glass substrates were formed using electrochemical deposition with different electrolyte concentrations. X-ray photoelectron spectroscopy spectra showed Zn $2p_{3/2}$, Zn $2p_{1/2}$, and O 1s peaks of ZnO samples, indicative of the formation of ZnO nanodisks. Scanning electron microscopy images showed that the density of the ZnO nanodisks increased with increasing electrolyte concentration. X-ray diffraction patterns showed that the intensities corresponding to the (100), (002), and (101) peaks for the ZnO nanodisks with the wurtzite structures increased with increasing electrolyte concentration, indicative of the preferential formation of the ZnO nanodisks. Photoluminescence spectra at 300 K for ZnO nanodisks showed that the dominant PL peak intensity of the near band-edge emissions decreased with increasing electrolyte concentration.

Key words: ZnO nanodisks, Electrochemical deposition, Electrolyte concentration, Structural properties, Optical properties.

Introduction

Semiconductor nanostructures have been particularly attractive because of interest in both investigations of fundamental physical properties [1] and potential applications in electronic and optoelectronic devices operating at lower currents and higher temperatures [2]. Promising applications of nanostructures in next-generation electronic and optoelectronic devices have driven extensive efforts to form various types of nanostructures, such as nanorods [3], nanowires [4], nanobelts [5], and nanotubes [6]. Among the various types of nanostructures, ZnO nanostructures have been currently receiving considerable attention due to their promising applications in light-emitting diodes [7], photodetectors [8], lasers [9], solar cells [10], and memories [11] because they have wide energy gaps with unique physical properties of large exciton binding energies and excellent chemical stabilities [12]. Even though ZnO nanorods and nanowires have been the most extensively studied structures, relatively little work has been performed on ZnO nanodisks in comparison with ZnO nanorods and nanowires because of the delicate problems encountered in the growth process. Furthermore, ZnO nanodisks have emerged as promising candidates for potential applications in light emitters, photodetectors, energy storage systems, chemical and biological sensors, and solar cells due to their high ratio of the surface to the volume [13]. Even though some studies concerning the formation and physical properties of ZnO nanostructures have been performed, systematic studies on the effect of electrolyte concentration on the structural and the optical properties of ZnO nanodisks formed on indium-tin-oxide (ITO) coated glass substrates grown by the electrochemical deposition (ECD) method are necessary to improve device efficiency.

This paper reports data on the effect of electrolyte concentration on the structural and optical properties of ZnO nanodisks formed on ITO-coated glass substrates using the ECD method. X-ray photoelectron spectroscopy (XPS) measurements were carried out to investigate the stoichiometry of the nanomaterials. Scanning electron microscopy (SEM) and X-ray diffraction (XRD) measurements were performed to clarify the structural properties of ZnO nanodisks formed with different electrolyte concentrations. Photoluminescence (PL) measurements were performed to investigate the optical properties of the ZnO nanodisks.

Experimental

ZnO nanodisks used in this study were formed on ITO-coated glass substrates using a ECD method. The resistivity of the ITO film was 17 Ω/square. The ZnO nanodisks were formed resulting from the reduction of dissolved molecular oxygen in a zinc nitrate solutions [14]. The electrochemical reduction of oxygen molecules generates from the combination between the precursor and the current of the cathode [15]. The ECD equipment consisting of three-electrode electrochemical cells with

*Corresponding author:
Tel : +82-2-2220-0354
Fax: +82-2-2292-4135
E-mail: twk@hanyang.ac.kr

an ITO cathode acting as a working electrode, a Pt electrode acting as a counter electrode, and a saturated calomel electrode (SCE) acting as a reference electrode was used to deposit the ZnO nanodisks. The density and the deposition efficiency of ZnO nanodisks were controlled by using the growth conditions of ECD. The electrolyte was $Zn(NO_3)_2 \cdot 6H_2O$ at various concentrations and 0.1 M KCl as a supporting electrolyte. Firstly, after high-purity ITO-coated glass substrates were rinsed with a mixture of methanol and deionized water in an ultrasonic cleaner, they were immersed into the reaction solution at 27 °C. The $Zn(NO_3)_2 \cdot 6H_2O$ and KCl (0.1 M) were dissolved in 200 ml deionized water. The KCl and the $Zn(NO_3)_2 \cdot 6H_2O$ act as a supporting precursor and a Zn^{2+} precursor, respectively. The concentrations of $Zn(NO_3)_2 \cdot 6H_2O$ solutions were 15, 30, 45, 60 and 75 mM. A solution temperature of 75 °C was maintained in deionized water under a constant applied voltage of -1.1 V for 2 h. The rapid thermal annealing process was performed in air at 400 °C for 2 minutes after the ZnO nanodisks formed were thoroughly cleaned using deionized water to eliminate residual salts, and dried in air at 50 °C for 5 minutes.

XPS measurements on the samples were performed using a VG Multilab ESCA 2000 system with a monochromated Mg K_α X-ray source (1253.6 eV). All the spectra obtained were calibrated to a C 1s electron peak at 284.5 eV. Field-emission SEM measurements were performed using a JSM-6330F. XRD measurements were carried out using a Rigaku D/MAX-2500 diffractometer meter with Cu K_α radiation, which was operated at a scanning speed of 5 °/min for a 2θ range between 20 ° and 70 °. The voltage and the current of the X-ray tube were set at 40 kV and 100 mA, respectively. The PL measurements were carried out using a 50-cm monochro-mator equipped with an RCA 31034 photomultiplier tube. The excitation source was the 325-nm line of a He-Cd laser, and the sample temperature was kept at 300 K.

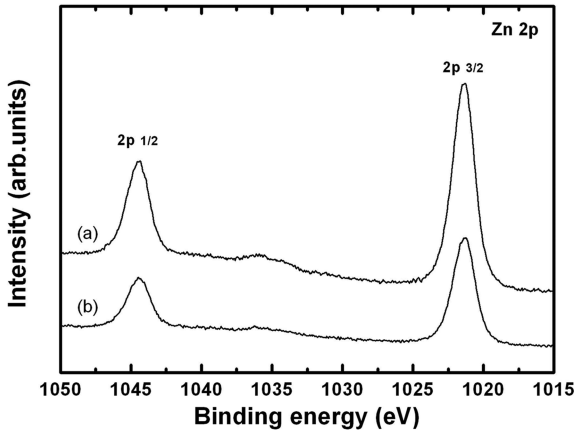

Fig. 1. Zn 2*p* X-ray photoelectron spectroscopy core-level spectra of ZnO nanodisks formed on ITO-glass substrates with electrolyte concentrations of (a) 45 and (b) 60 mM.

Results and Discussion

Figs. 1 and 2 show XPS spectra of ZnO nanodisks formed by using electrolyte concentrations of 45 and 60 mM. The Zn 2*p* core-level photoemission (PE) spectra of ZnO nanodisks on the ITO-glass substrates are shown in Fig. 1. A shoulder around 1021.5 eV corresponds to the oxidation state of Zn $2p_{3/2}$, which is in reasonable agreement with ZnO bulk. While the peaks of the Zn $2p_{1/2}$ and $2p_{3/2}$ spectra clearly verify the presence of Zn^{2+} ions in the nanodisks, any surface metal reduction did not appear. The asymmetric O 1*s* core-level PE spectra of ZnO nanodisks formed with electrolyte concentrations of 45 mM are shown in Fig. 2(a). The peaks at 530 eV of phase 2 and 531.2 eV of phase 1 are coherently fitted by two Gaussian components. The O 1*s* binding energy of the phase 2 peak is attributed to the Zn-O bonds, which is identified from the Zn 2*p* spectra, indicating that the material formed is ZnO. The value of the O 1s binding energy of the phase 2 is attributed to the O^2 ions in the wurtzite structure of the hexagonal Zn^{2+} ion array, which are surrounded by zinc atoms with the full supplement of the nearest-neighbor O^2 ions. However, the value of the O 1*s* binding energy of the phase 1 is larger than that of the O 1*s* binding energy of the phase 2 by 1.0 eV, and is typically attributed to the O-H bonds or the chemisorbed oxygen on the surface of

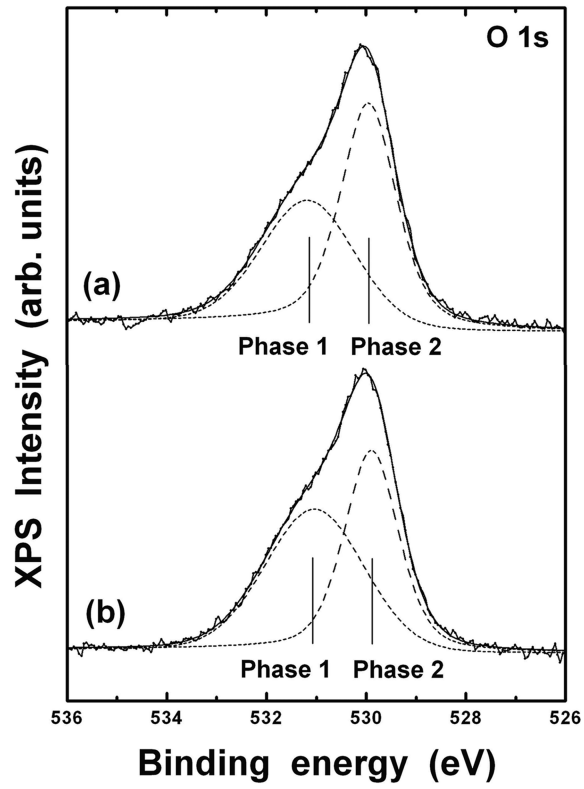

Fig. 2. O 1*s* X-ray photoelectron spectroscopy core-level spectra of ZnO nanodisks with electrolyte concentrations of (a) 45 and (b) 60 mM. The vertical lines indicate the positions of the binding energies of the Gaussian distribution functions.

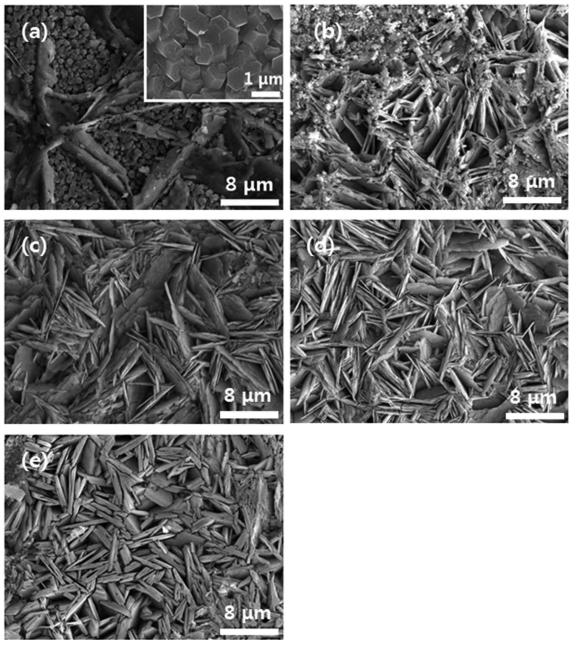

Fig. 3. Scanning electron microscopy images of ZnO nanodisks formed on the ITO-glass substrates at 75 °C with electrolyte concentrations of (a) 15, (b) 30, (c) 45, (d) 60 and (e) 75 mM.

the ZnO nanodisks [16]. The O 1*s* core-level PE spectra of ZnO nanodisks formed by an electrolyte concentration of 60 mM shown in Fig. 2(b) is similar to the O 1*s* core-level PE spectra of ZnO nanodisks formed by an electrolyte concentration of 45 mM. Therefore, Figs. 1 and 2 demonstrate that ZnO nanodisks are well formed, regardless of the electrolyte concentration.

Fig. 3 shows the SEM images of ZnO nanodisks formed on ITO-coated glass substrates with different electrolyte concentrations. Fig. 3(a) shows that few ZnO nanodisks are formed with a low electrolyte concentration of 15 mM. ZnO nanorods mixed with ZnO nanodisks are vertically aligned, as shown in the inset of Fig. 3(a), and their diameters are approximately 500 nm [17]. Figs. 3(b), 3(c), and 3(d) show that the density of the ZnO nanodisks increases with an increase in the electrolyte concentration. When the ZnO nanodisks are deposited with a high electrolyte concentration of 75 mM, some ZnO nanodisks are changed into ZnO nanowalls. The density of the ZnO nanodisks is varied by the changing electrolyte concentration [18].

Fig. 4 shows XRD patterns of the ZnO nanodisks formed using different electrolyte concentrations of 15, 30, 45, 60, and 75 mM. The XRD patterns show that the ZnO nanodisks have the wurtzite structure with cell parameters of a = 3.250 Å and c = 5.207 Å, which are in reasonable agreement with the literature values (JCPDS card no. 36-1451). The strong peaks at 31.8 °, 34.5 °, and 36.3 ° corresponds to the (100), (002), and (101) planes of the wurtzite ZnO nanodisks. When ZnO nanostructures are formed with a electrolyte concentration of 15 mM, few ZnO nanodisks are formed near the top region of the nanorods, as shown

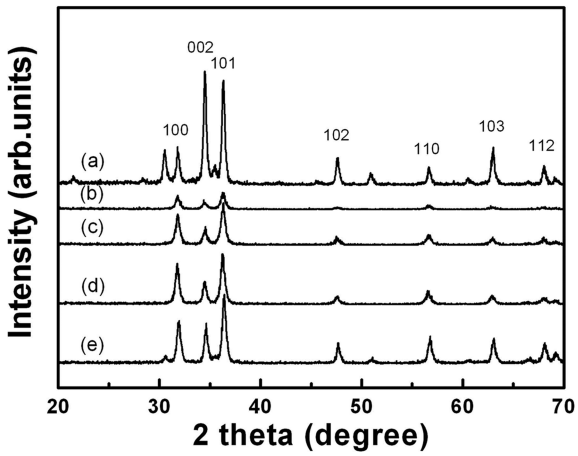

Fig. 4. X-ray diffraction patterns of ZnO nanodisks formed on ITO-glass substrates at 75 °C with electrolyte concentrations of (a) 15, (b) 30, (c) 45, (d) 60, and (e) 75 mM.

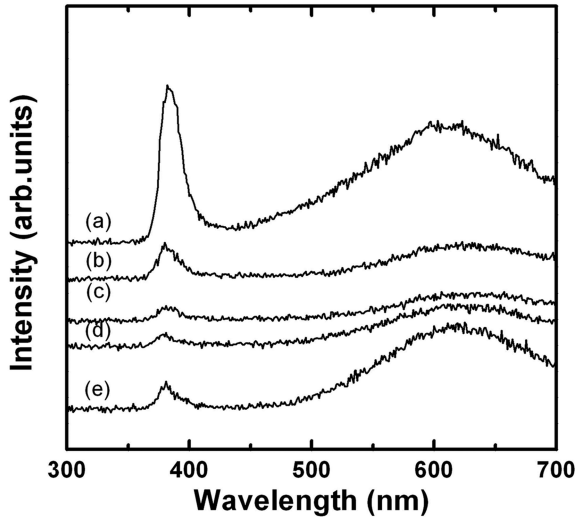

Fig. 5. Photoluminescence spectra of ZnO nanodisks formed on the ITO-glass substrates at 75 °C with electrolyte concentrations of (a) 15, (b) 30, (c) 45, (d) 60 and (e) 75 mM.

in Fig. 3(a). The strong intensity of the (002) peak corresponding to the ZnO nanodisks is similar to that of the ZnO nanorods, indicative of the preferentially aligned c-axis of the ZnO nanodisks. The relatively smaller intensities of (100) and (101) peaks are attributed to a small fraction of the nonaligned nanodisks [18]. ZnO nanodisks formed by an electrolyte concentration of 30 mM exist near the top of nanorods, as shown in Fig. 4(b). The relative XRD intensities of the peaks are decreased because few ZnO nanodisks were formed on the nanorods. Figs. 4(c), 4(d), and 4(e) show the ZnO nanodisks formed by the electrolyte concentration of 45, 60, and 75 mM. The XRD intensities corresponding to the (100), (002), and (101) peaks for the ZnO nanodisks increased with an increase in the electrolyte concentration, indicative of the preferential formation of the ZnO nanodisks, as shown in Figs. 4(b), 4(c), 4(d), and 4(e).

Fig. 5 shows the PL spectra at 300 K for the ZnO nanodisks formed with different electrolyte concentrations of 15, 30, 45, 60, and 75 mM. PL spectra for the ZnO nanodisks at 300 K show two emission bands. A dominant peak in the near-ultraviolet region attributed to free excitonic recombination corresponds to near band-edge emissions [19], and a broad band emission in the visible region is related to deep-level intrinsic defect emission in ZnO nanodisks. The photogenerated holes are trapped by the surface state of oxygen defects [20]. The shapes of PL spectra in terms of the intensity ratio of the ultraviolet to visible bands are significantly affected by the morphology of the ZnO nanodisks due to the variations of electrolyte concentrations.

Conclusions

The effect of electrolyte concentration on the structural and optical properties of ZnO nanodisks formed on ITO-coated glass substrates using ECD with different electrolyte concentrations was investigated. XPS spectra showed Zn $2p_{3/2}$, Zn $2p_{1/2}$, and O 1s peaks of ZnO samples, indicative of the formation of ZnO nanodisks. SEM images showed that the density of the ZnO nanodisks increased with an increase in the electrolyte concentration. XRD patterns showed that the formed ZnO nanodisks had the wurtzite structure and that the intensities corresponding to the (100), (002), and (101) peaks for the ZnO nanodisks increased with an increase in the electrolyte concentration, indicative of the preferential formation of the ZnO nanodisks. PL spectra at 300 K for ZnO nanodisks showed that the dominant PL peak intensity of the near band-edge emissions decreased with an increase in the electrolyte concentration. These results can help to improve an understanding of the effect of the electrolyte concentration on the structural and optical properties of ZnO nanodisks.

Acknowledgment

This research was supported by Basic Science Research Program through the National Research Foundation of Korea (NRF) funded by the Ministry of Education, Science and Technology (2011-0025491). The work of J. Y. Kim was conducted during the sabbatical year by Kwangwoon University in 2012.

References

1. M. Law, D.J. Sirbuly, J.C. Johnson, J. Goldberger, R.J. Saykally, and P.D. Yang, Science 305 (2004) 1269-1273.
2. R. Yan, D. Gargas, and P. Yang, Nat. Photonics 3 (2009) 569-576.
3. Y.B. Tang, Z.H. Chen, H.S. Song, C.S. Lee, H.T. Cong, H. M. Cheng, W.J. Zhang, I. Bello, and S.T. Lee, Nano Lett. 8 (2008) 4191-4195.
4. M.P. Zach, K.H. Ng, and R.M. Penner, Science 290 (2000) 2120-2123.
5. Z.W. Pan, Z.R. Dai, and Z.L. Wang, Science 291 (2001) 1947-1949.
6. N. Wang, Z.K. Tang, G.D. Li, and J.S. Chen, Nature 408 (2000) 50-51.
7. D.I. Son, C.H. You, W.T. Kim, and T.W. Kim, Nanotechnology 20 (2009) 365206-1-365206-5.
8. Y.H. Leung, Z.B. He, L.B. Luo, C.H. A. Tsang, N.B. Wong, W.J. Zhang, and S.T. Lee, Appl. Phys. Lett. 96 (2010) 053102-1-053102-3.
9. H. Zhu, C.X. Shan, B. Yao, B.H. Li, J.Y. Zhang, Z.Z. Zhang, D.X. Zhao, D.Z. Shen, X.W. Fan, Y.M. Lu, and Z. K. Tang, Adv. Mater. 21 (2009) 1613-1617.
10. J. Liu, S. Wang, Z. Bian, M. Shan, and C. Huang, Appl. Phys. Lett. 94 (2009) 173107-1-173107-3.
11. D.Y. Yun, J.K. Kwak, J.H. Jung, T.W. Kim, and D.I. Son, Appl. Phys. Lett. 95 (2009) 143301-1-143301-3.
12. Z.L. Wang, Mater. Sci. Eng. R 64 (2009) 33-71.
13. L.W. Ji, S.M. Peng, Y.K. Su, S.J. Young, C.Z. Wu, and W.B. Cheng, Appl. Phys. Lett. 94 (2009) 203106-1-203106-3.
14. R. Konekamp, K. Boedecker, M.C. Lux-Steiner, M. Poschenrieder, F. Zenia, C. Levy-Clement, and S. Wagner, Appl. Phys. Lett. 77 (2000) 2575-2577.
15. S. Strbac and R.R. Adzic, Electrochim. Acta 41 (1996) 2903-2908.
16. B. Yang, A. Kumar, H. Zhang, P. Feng, R.S. Katiyar, and Z. Wang, J. Phys. D: Appl. Phys. 42 (2009) 045415-1-045415-7.
17. C.Z. Zhang, H. Gao, D. Zhang, and X.T. Zhang, Chin. Phys. Lett. 25 (2008) 302-305.
18. D. Pradhan and K.T. Leung, Langmuir 24 (2008) 9707-9716.
19. H.J. Ko, Y.F. Chen, T. Yao, K. Miyajima, A. Yamamoto, and T. Goto, Appl. Phys. Lett. 77 (2000) 537-539.
20. C.X. Xu, G.P. Zhu, J. Kasim, S.T. Tan, Y. Yang, X. Li, Z.X. Shen, and X.W. Sun, Curr. Appl. Phys. 9 (2009) 573-576.